1   **Durable SARS-CoV-2 B cell immunity after mild or severe disease**

2   Clinton O. Ogega[1], Nicole E. Skinner[1], Paul W. Blair[1], Han-Sol Park[2], Kirsten Littlefield[2],

3   Abhinaya Ganesan[2], Pranay Ladiwala[3], Annukka AR Antar[1], Stuart C. Ray[1], Michael J.

4   Betenbaugh[3], Andrew Pekosz[2], Sabra L. Klein[2], Yukari C. Manabe[1], Andrea L. Cox[1,2], and

5   Justin R. Bailey[1]*

6   **Affiliations**:

7   [1]Division of Infectious Diseases, Department of Medicine, Johns Hopkins University School of

8   Medicine, Baltimore, Maryland, USA.

9   [2]W. Harry Feinstone Department of Molecular Microbiology and Immunology, The Johns

10   Hopkins Bloomberg School of Public Health, Baltimore, Maryland, USA.

11   [3]Advanced Mammalian Biomanufacturing Innovation Center, Department of Chemical and

12   Biomolecular Engineering, Johns Hopkins University, Baltimore, Maryland, USA.

13

14   **Key words**: SARS-CoV-2, COVID-19, neutralizing antibody, memory B cell

15   ***Address correspondence to:**

16   Justin R. Bailey, MD, PhD
17   855 N. Wolfe Street
18   Rangos Building, Suite 520
19   Baltimore MD 21205, USA
20   Phone: 410-614-6087
21   Email: jbailey7@jhmi.edu

22

23   **Conflict of interest statement.** The authors declare that they have no conflicts of interest.

24 **Abstract**

25 Multiple studies have shown loss of SARS-CoV-2 specific antibodies over time after infection,

26 raising concern that humoral immunity against the virus is not durable. If immunity wanes

27 quickly, millions of people may be at risk for reinfection after recovery from COVID-19.

28 However, memory B cells (MBC) could provide durable humoral immunity even if serum

29 neutralizing antibody titers decline. We performed multi-dimensional flow cytometric analysis of

30 S protein receptor binding domain (S-RBD)-specific MBC in cohorts of ambulatory COVID-19

31 patients with mild disease, and hospitalized patients with moderate to severe disease, at a median

32 of 54 (39-104) days after onset of symptoms. We detected S-RBD-specific class-switched MBC

33 in 13 out of 14 participants, including 4 of the 5 participants with lowest plasma levels of anti-S-

34 RBD IgG and neutralizing antibodies. Resting MBC (rMBC) made up the largest proportion of

35 S-RBD-specific class-switched MBC in both cohorts. FCRL5, a marker of functional memory

36 when expressed on rMBC, was dramatically upregulated on S-RBD-specific rMBC. These data

37 indicate that most SARS-CoV-2-infected individuals develop S-RBD-specific, class-switched

38 MBC that phenotypically resemble germinal center-derived B cells induced by effective

39 vaccination against other pathogens, providing evidence for durable B cell-mediated immunity

40 against SARS-CoV-2 after recovery from mild or severe COVID-19 disease.

41

42 **Introduction**

43 We are in the midst of an ongoing global pandemic caused by a novel coronavirus, SARS-CoV-

44 2. COVID-19, the disease caused by SARS-CoV-2, can cause pulmonary inflammation, acute

45 respiratory distress syndrome (ARDS), respiratory failure, and death. Despite the high morbidity

46 and mortality caused by COVID-19, the majority of SARS-CoV-2-infected individuals recover

47 and survive (1, 2). Following recovery, the durability of immunity against SARS-CoV-2 remains

48 unclear. Durability of immunity is critical to mitigate the risk of reinfection for millions of

49 people who have recovered or will recover from COVID-19.

50

51 After clearance of an infection or effective vaccination, phenotypically distinct B cell

52 populations contribute to short- and long-term humoral immunity. Short-lived antibody-secreting

53 cells (ASC) in blood and secondary lymphoid organs release antibodies into the circulation for

54 weeks to months. Durable humoral immunity (lasting months to years) is mediated by bone

55 marrow-resident, long-lived ASC and by memory B cells (MBC), which rapidly proliferate and

56 differentiate into ASC in response to antigen re-challenge. Multiple studies have now

57 demonstrated that serum antibody titers against SARS-CoV-2 wane and can even become

58 undetectable after resolution of infection (3-6), likely reflecting a decline in short-lived ASC

59 populations over time. Although other emerging reports have demonstrated more durable serum

60 antibody responses (7-10), concerns remain that individuals who have recovered from COVID-

61 19 may not maintain adequate immunity against reinfection. Individuals with mild COVID-19

62 disease generally mount lower titer antibody responses against the virus than those with severe

63 disease (3, 10), raising particular concern that those who recover from mild infection are not

64 protected against reinfection. If present and functional, MBC could provide durable humoral

65   immunity even after the loss of detectable serum antibody titers, as has been demonstrated after

66   vaccination against viruses like hepatitis B virus (11, 12). However, Kaneko et al. showed a

67   dramatic loss of germinal centers during acute COVID-19, raising concern that T cell dependent,

68   durable, class-switched SARS-CoV-2-specific MBC responses may not reliably develop after

69   SARS-CoV-2 infection (13).

70

71   Little is known about the frequency and phenotype of SARS-CoV-2-specific MBC that develop

72   in response to either severe or mild infection. B cells specific for the SARS-CoV-2 Spike (S)

73   protein have been isolated from individuals with very low antibody titers, but the relatively low

74   frequency of these cells has thus far limited further characterization (14). We developed a highly

75   sensitive and specific flow cytometry-based assay to quantitate circulating SARS-CoV-2 S

76   protein receptor binding domain (S-RBD)-specific B cells, and a cell surface phenotyping panel

77   to characterize these cells. We focused on S-RBD-specific B cells because most virus-

78   neutralizing human monoclonal antibodies target this domain (14-18). Neutralizing activity has

79   been associated with protection against reinfection by other coronaviruses (19-22), and

80   protection against challenge in animal models of SARS-CoV-2 infection (23, 24). Therefore, S-

81   RBD-specific B cells are likely to be the cells responsible for production of protective

82   neutralizing antibodies upon re-exposure.

83

84   Classical markers applied to these S-RBD-specific B cells allowed us to identify B cell lineages

85   including non-class-switched B cells, class-switched ASC, class-switched resting (classical)

86   MBC (rMBC), activated MBC (actMBC), atypical MBC (atyMBC), and intermediate MBC

87   (intMBC). Additional subpopulations were identified by staining for a chemokine receptor

88   (CXCR5), and potential inhibitory or activating receptors (FCRL5, CD22, and BTLA). Among

89   the cell surface regulatory molecules, FCRL5 expression is of particular interest, since its

90   expression on atyMBC has been associated with B cell dysfunction in chronic infections like

91   HIV-1 and hepatitis C virus (25). In contrast, it is also upregulated on long-lived antigen-specific

92   rMBC that develop after effective vaccination against influenza and tetanus (26, 27). This

93   FCRL5+ rMBC population prefentially expands and forms plasmablasts on antigen re-challenge,

94   indicating that FCRL5 expression on antigen-specific rMBC is a marker of effective long-lived

95   B cell-mediated immunity.

96

97   To investigate the potential for durable B cell immunity after SARS-CoV-2 infection, we

98   analyzed S-RBD-specific B cells in ambulatory COVID-19 patients with mild disease and

99   hospitalized patients with moderate to severe disease. We detected S-RBD-specific non-class-

100   switched B cells, S-RBD-specific class-switched ASC, and/or S-RBD-specific class-switched

101   MBC in all participants, regardless of their serum antibody titers or disease severity. We

102   analyzed the frequencies of these S-RBD-specific B cell populations, and of S-RBD-specific

103   MBC subsets, including rMBC, intMBC, actMBC, and atyMBC. By also quantifying cell surface

104   molecules CD38, FCRL5, CD22, BTLA, and CXCR5 on these MBC populations and subsets,

105   we identified a phenotypic profile of S-RBD-specific class switched MBC that was consistent

106   with functional, durable B cell immunity.

107

108

109 **Results**

110 **Selection of study participants.**

111 B cells were obtained from participants with mild COVID-19 disease, moderate to severe

112 disease, and from healthy COVID-19 negative controls (Table 1). Participants with mild

113 COVID-19 disease who never required hospitalization or supplemental oxygen were identified in

114 a previously described cohort of ambulatory patients (28). Symptoms in this cohort were tracked

115 using a FLU-PRO score calculated from a participant survey, as previously described (28). To

116 ensure that participants with mild disease were included in this study, a group of seven

117 participants was selected with a median peak FLU-PRO score below the median peak score for

118 the entire ambulatory cohort (FLU-PRO median (range)=0.09 (0.0-0.38) vs. 0.25 (0.0-1.63)).

119 Seven additional participants with moderate to severe COVID-19 disease were selected from a

120 second cohort of hospitalized patients (29), matched with the mild disease participants based on

121 time since onset of symptoms at the time of blood sampling (median (range) time since symptom

122 onset in days: ambulatory=61 (45-68); hospitalized=46 (39-104)). Peak supplemental oxygen

123 support in hospitalized participants ranged from 2L via nasal cannula to mechanical ventilation.

124 At the time of blood sampling for this study, five of the hospitalized participants had been

125 discharged, and two remained hospitalized with critical illness. Hereafter, ambulatory,

126 hospitalized, and healthy groups will be referred to as "mild", "severe", and "healthy",

127 respectively.

128 **Quantitation of S-RBD-specific B cells**.

129 A flow cytometry antibody panel was designed to identify non-class switched B cells (CD3-,

130 CD19+, IgD/IgM+), class switched memory B cells (MBC) (CD3-, CD19+, IgM-, IgD-,

131   CD38+/- (excluding ++), CD138-) and class switched antibody secreting cells (ASC) (CD3-,

132   CD27+, CD19+/-, IgM-, IgD-, CD38++) (Supp. Figure 1). The frequency of all non-class

133   switched B cells, class switched MBC, or class switched ASC among single viable lymphocytes

134   was not significantly different between healthy, mild, and severe groups, but there was a trend

135   toward greater frequency of class-switched ASC in the severe group compared to mild and

136   healthy groups (Figure 1A). As we defined these three B cell populations, we used a 6x-histidine

137   tagged, soluble S-RBD protein followed by anti-His Alexa Fluor 647-conjugated antibody to

138   stain cells expressing S-RBD-specific antibodies on their surface (Figure 1B and Supplemental

139   Figure 1). We quantitated the frequency of these S-RBD-specific cells among non-class switched

140   B cells, class switched ASC, and class switched MBC (Figure 1C). Four of seven (57%) mild

141   and seven of seven (100%) severe participants had a frequency of S-RBD-specific non-class

142   switched B cells above the true positive threshold set using the healthy group. The frequency of

143   these cells did not differ significantly between the mild and severe groups. Four of seven (57%)

144   mild and four of seven (57%) severe participants had a frequency of S-RBD-specific class

145   switched ASC above the true positive threshold. The frequency of these cells also did not differ

146   significantly between the mild and severe groups. Six of seven (86%) mild and seven of seven

147   (100%) severe participants had a frequency of S-RBD-specific class switched MBC above the

148   true positive threshold. The single individual without detectable S-RBD-specific class switched

149   MBC was asymptomatic throughout infection (peak FLU-PRO=0.0). Frequency of S-RBD-

150   specific class switched MBC was significantly higher in severe participants than in mild

151   participants (mean S-RBD+ frequency 0.85% vs. 0.20%, p=0.004). Taken together, these data

152   demonstrate that S-RBD-specific cells could be detected among non-class switched B cells and

153   class switched ASC in most SARS-CoV-2-infected participants, and S-RBD-specific class

154   switched MBC could be detected in thirteen of fourteen participants. S-RBD-specific cells were

155   significantly more frequent among class switched MBC from the severe group relative to the

156   mild group.

157   **Detectable S-RBD-specific MBC despite low levels of anti-S-RBD IgG and neutralizing**

158   **antibodies in plasma.**

159   Given concerns that low or waning plasma titers of neutralizing antibodies in some individuals

160   indicate a lack of a durable humoral response, we were interested in evaluating whether COVID-

161   19 participants with low levels of plasma anti-S-RBD IgG and low neutralizing antibody levels

162   had detectable S-RBD-specific MBC in circulation. S-RBD binding IgG was measured using

163   serial dilutions of plasma in an ELISA, and neutralizing antibodies were measured with serial

164   dilutions of plasma in a microneutralization assay using replication competent SARS-CoV-2

165   virus (10). Curves were fit to these data, and area under the curve (AUC) values calculated. Anti-

166   S-RBD IgG and neutralization AUC values each varied over a wide range across study subjects

167   (1e2.7-1e4.9 and 1e0.8-1e3.0, respectively). As expected based on prior studies (3, 10), there

168   was a trend toward higher anti-S-RBD IgG and neutralization AUC values in the severe group

169   relative to the mild group, although these differences were not statistically significant, likely due

170   to the small number of subjects (Figure 2A-B). We next evaluated whether we could detect S-

171   RBD-specific cells among class switched MBC of participants with low, intermediate, or high

172   levels of plasma anti-S-RBD IgG (Figure 2C) or low, intermediate, or high levels of neutralizing

173   antibodies (Figure 2D). We detected S-RBD-specific class switched MBC above the nonspecific

174   background frequency in 4 of 5 participants with the lowest IgG and neutralization AUCs, 5 of 5

175   with intermediate AUCs, and 4 of 4 with highest AUCs. The single individual without detectable

176   S-RBD-specific class switched MBC had the lowest levels of plasma anti-S-RBD IgG

177   (AUC=1e2.7) and neutralizing antibodies (AUC=1e0.8) in the study. There was a non-significant

178   trend toward higher frequencies of RBD specific cells among class switched MBC in the higher

179   AUC IgG and higher neutralizing antibody AUC groups relative to the lowest AUC groups.

180   Overall, these data show that S-RBD-specific class switched MBC were detectable in the

181   circulation of most infected individuals, including the majority of subjects with low levels of

182   plasma anti-S-RBD IgG and neutralizing antibodies.

183   **UMAP analysis of class switched MBC surface markers.**

184   To further characterize the phenotypes of S-RBD-specific and nonspecific class switched MBC

185   in healthy, mild, or severe COVID-19 patients, we studied surface expression of CD21, CD27,

186   FCRL5, CXCR5, CD22, BTLA, and CD38. CD21 and CD27 expression allow separation of

187   MBC into intermediate MBC (intMBC, CD21+ CD27-), resting MBC (rMBC, CD21+, CD27+),

188   activated MBC (actMBC, CD21- CD27+), and atypical MBC (atyMBC, CD21- CD27-) subsets.

189   B- and T- lymphocyte attenuator (BTLA) or CD272 and CD22/Siglec2 are immune cell

190   inhibitory receptors with cytoplasmic immunoreceptor tyrosine-based inhibition motifs (ITIMs)

191   (30-33), while FCRL5 has two ITIMs and one immunoreceptor tyrosine-based activation motif

192   (ITAM) (34, 35). C-C chemokine receptor type 5 (CXCR5) is a germinal center homing receptor

193   that is generally down-regulated after cells have undergone class switching and somatic

194   hypermutation (36, 37). CD38 has relatively undefined functional significance, but it is negative

195   on "late" class-switched MBC and positive on "early" class switched MBC that emerged more

196   recently from germinal center reactions (38).

197   We first analyzed a UMAP projection of all class switched MBC from healthy, mild, and severe

198   groups generated based on binding of S-RBD and expression of CD21, CD27, CD38, CD22,

199   FCRL5, CXCR5, and BTLA (Figure 3A). This UMAP identified a clear segregation of co-

200   mingled mild and severe S-RBD+ cells from RBD- and healthy donor cells. From this UMAP

201   clustering projection, we extrapolated multigraph color mapping of the receptors with observed

202   differential expression of all surface markers except BTLA (Figure 3B). To determine whether

203   there was any shift in expression of these markers between study groups, we overlayed

204   expression histograms of all the surface receptors of healthy, mild S-RBD-, mild S-RBD+,

205   severe S-RBD-, and severe S-RBD+ class switched MBC (Figure 3C). Again, there was no

206   observable shift in the expression of BTLA. For all study groups, there was a bimodal

207   distribution of CD21 expression, indicating that both CD21+ (intMBC and rMBC) and CD21-

208   (actMBC and atyMBC) MBC subsets were present. For both mild and severe S-RBD+ MBC, we

209   observed a shift toward increased expression of CD22 and FCRL5 and downregulation of

210   CXCR5 compared to healthy and S-RBD- populations. For CD38, we observed upregulation in

211   mild and severe S-RBD+ MBC and downregulation in mild and severe S-RBD- MBC compared

212   to healthy participants.

213   **Quantifying subsets of S-RBD nonspecific and S-RBD-specific class switched MBC**

214   To better understand the functional phenotypes of the S-RBD-specific MBC identified in both

215   mild and severe groups, we compared the frequencies of intMBC, rMBC, actMBC, and atyMBC

216   among S-RBD-specific and S-RBD nonspecific class switched MBC at the level of individual

217   participants (Figure 4). MBC subsets identified based on CD21 and CD27 expression have

218   notably different phenotypes (38). Classical MBC, also called rMBC, persist for months to years

219   and respond to antigen re-challenge by proliferating and differentiating into antibody-producing

220   ASC. ActMBC are cells that recently left germinal centers and are already primed to become

221   antibody secreting plasma cells (39). AtyMBC are generally thought to be poorly functional, and

222   are present at higher frequencies in chronic infections like HIV-1, hepatitis C virus, tuberculosis,

223   or malaria (25, 40, 41). AtyMBC were also found to be more frequent among bulk (not antigen

224   specific) MBC during acute SARS-CoV-2 infection (42). IntMBC likely represent a transitional

225   state between MBC subsets.

226   S-RBD-specific class switched MBC from two participants were not included in these or

227   subsequent analyses, either because they did not have detectable S-RBD-specific class switched

228   MBC frequency above background (subject M5), or because absolute cell numbers were low

229   given severe lymphopenia (subject S3). S-RBD nonspecific MBC were adequately abundant in

230   all participants to allow their inclusion in all analyses (see Methods). There were no statistically

231   significant differences in the frequencies of intMBC, rMBC, or atyMBC subsets among S-RBD-

232   specific or S-RBD nonspecific class switched MBC from healthy, mild or severe participants

233   (Figure 4). In contrast, actMBC were significantly more frequent among both S-RBD

234   nonspecific and S-RBD-specific MBC populations in severe participants compared to healthy

235   and mild participants (e.g. mean frequency of severe S-RBD+ MBC vs. healthy S-RBD- MBC,

236   16.09% vs. 5.53%, p=0.01) (Figure 4C). This likely represents greater ongoing immune

237   activation in the severe infection group relative to the healthy and mild groups and is also

238   consistent with the observed trend toward higher frequency of ASC in the severe group (Figure

239   1A). Overall, these data demonstrate an expected distribution of S-RBD-specific cells among

240   MBC subsets, with the largest proportion of S-RBD-specific class switched MBC in both mild

241   and severe groups falling in the rMBC subset.

242   **Expression of activating or inhibitory surface markers on class switched MBC and MBC**

243   **subsets.**

244   To further investigate the differential expression of surface markers that we observed in the

245   UMAP projections and histograms of grouped samples, we compared expression of FCRL5,

246   CXCR5, CD22, and CD38 at the level of individual participants between healthy, mild S-RBD-,

247   mild S-RBD+, severe S-RBD-, and severe S-RBD+ groups (Figure 5). BTLA expression was not

248   included in this analysis given no differential expression in the UMAP. We found that FCRL5

249   was dramatically upregulated in mild S-RBD+ MBC relative to healthy cells, mild S-RBD- cells,

250   and severe S-RBD+ cells (p=<0.0001, 0.003, and 0.01, respectively). FCRL5 was also

251   upregulated to a lesser, but still significant extent on severe S-RBD+, mild S-RBD-, and severe

252   S-RBD- MBC relative to healthy MBC (p=0.01, 0.03, and 0.04, respectively) (Figure 5A). The

253   frequency of CXCR5+ cells among class switched MBC was not significantly different between

254   the groups, although it was downregulated in 3 of 6 participants in both mild and severe groups

255   (Figure 5B) which could account for the shift observed in the histogram in Figure 3C. Since

256   CD22/siglec-2 is ubiquitously expressed on B cells, we analyzed its relative expression by

257   comparing mean fluorescence intensities (MFI). Compared to healthy controls, CD22 was

258   upregulated on mild S-RBD+ class switched MBC (p=0.04) (Figure 5C). Among class switched

259   MBC, CD38 expression did not differ significantly between SARS-CoV-2 infected and healthy

260   participants (Figure 5D).

261   Having observed upregulation of both FCRL5 and CD22, a trend toward downregulation of

262   CXCR5, and a trend toward upregulation of CD38 on S-RBD+ class switched MBC, we

263   analyzed expression of these surface markers on MBC subsets rMBC, intMBC, actMBC, and

264   atyMBC (Figure 6). As with total class switched RBD+ MBC, we found that FCRL5 was

265   dramatically upregulated on mild S-RBD+ rMBC relative to healthy rMBC, mild S-RBD-

266   rMBC, and severe S-RBD+ rMBC (p=<0.0001, <0.0001, and <0.0001, respectively). FCRL5

267   was also upregulated to a lesser, but still significant extent on severe S-RBD+ and mild S-RBD-

268   rMBC relative to healthy rMBC (p=0.02 and 0.01, respectively). CXCR5 was significantly

269   downregulated on mild S-RBD+ atyMBC relative to healthy atyMBC, mild S-RBD- atyMBC,

270   and severe S-RBD+ atyMBC (p=0.001, 0.003, and 0.001, respectively). CD22 was significantly

271   upregulated on mild S-RBD+ rMBC and intMBC relative to healthy cells (p=0.02 and 0.03,

272   respectively). CD38+ cells were significantly more frequent among mild S-RBD+ actMBC

273   relative to healthy actMBC and mild S-RBD- actMBC (p=0.007 and 0.01, respectively). Taken

274   together, these results indicate that FCRL5 was significantly upregulated on S-RBD-specific

275   rMBC in both mild and severe infection. In mild but not severe infection, CD22 was upregulated

276   on S-RBD-specific rMBC and intMBC, CXCR5 was downregulated on S-RBD-specific

277   atyMBC, and CD38 was upregulated on S-RBD-specific actMBC.

278

Discussion

To investigate the durability of B cell immunity after SARS-CoV-2 infection, we analyzed S-RBD-specific B cells in ambulatory COVID-19 patients with mild disease and hospitalized patients with moderate to severe disease, at a median of 54 days after onset of symptoms. We detected S-RBD-specific class-switched MBC in 13 out of 14 participants, including 4 of the 5 participants with lowest plasma levels of anti-S-RBD IgG and neutralizing antibodies. The largest proportion of S-RBD-specific class-switched MBC in both cohorts were rMBC. AtyMBC, which tend to be poorly functional, were a minor population. FCRL5 was upregulated on S-RBD-specific rMBC after severe infection, and upregulated even more dramatically after mild infection.

These findings are of particular interest given the observation of Kaneko et al. of a dramatic loss of germinal centers in lymph nodes and spleens after SARS-CoV-2 infection (13). This observation would suggest that SARS-CoV-2-specific B cells in infected individuals lack T cell help and would therefore have reduced capacity to undergo class switching and transition to a resting memory phenotype. Our data indicate that despite this loss of germinal centers, T cell help is adequate to facilitate class switching of S-RBD-specific B cells, and transition of many of these cells to a resting state, regardless of disease severity. We did not measure the extent of somatic hypermutation of these B cells, but multiple groups have already demonstrated that human S-RBD-specific antibodies acquire enough somatic mutations to achieve very high affinity (14-18), again demonstrating that T cell help is adequate in most individuals.

A prior study by Oliviero et al. of bulk (not antigen-specific) MBC subsets during acute or convalescent COVID-19 found that atyMBC were expanded during acute infection, with atyMBC frequencies normalizing during convalescence (42). Our study extends that evaluation

302   by studying both S-RBD-specific and S-RBD nonspecific MBC. We found that S-RBD-specific

303   and S-RBD nonspecific atyMBC frequencies did not differ significantly from healthy controls,

304   but S-RBD-specific actMBC were expanded in severely infected individuals. The contrast of our

305   results with those of Oliviero et al. likely arise from differing timing after infection, and also by

306   our focus on antigen-specific MBC. The fact that atyMBC make up a small minority of S-RBD-

307   specific MBC provides further evidence that most S-RBD-specific MBC are normally functional.

308   It is interesting that the single individual without detectable S-RBD-specific class

309   switched MBC was asymptomatic throughout infection, and also had the lowest levels of anti-S-

310   RBD IgG and neutralizing antibodies in the study. It is possible that those with asymptomatic

311   disease, who tend to develop lower neutralizing antibody titers, may also develop lower

312   frequencies of class switched RBD-specific MBC. Given the low frequency of RBD specific

313   MBC across the cohort, we would need to analyze a larger number of PBMC to confirm with

314   confidence that this individual is truly negative for S-RBD-specific class switched MBC.

315   A limitation of this study is the lack of long-term longitudinal sampling of B cells after

316   infection, which would be required to prove that the S-RBD-specific MBC responses observed

317   here are truly durable. These studies will be pursued as longitudinal samples become available.

318   However, we have shown here that S-RBD-specific MBC in most infected individuals have a

319   phenotype that very closely resembles the phenotype of germinal center-derived MBC induced

320   by effective vaccination against influenza and tetanus. Of particular note is the upregulation of

321   FCRL5 on S-RBD-specific class switched rMBC after either mild or severe disease. FCRL5 is

322   expressed by most germinal center-derived MBC in plasmodium-infected mice, and these

323   FCRL5+ MBC differentiate into ASC on re-challenge (26). In addition, Kim et al. found that in

324   humans, presumably vaccinated against tetanus months to years prior, FCRL5 was upregulated

325   on tetanus specific rMBC (CD21+, CD27+) but not on bulk rMBC (26). Nellore et al. showed

326   similar results after influenza vaccination of humans, demonstrating that hemagglutinin (HA)-

327   specific, FCRL5+ MBC were induced by vaccination, and that these FCRL5+ MBC

328   preferentially differentiated into plasmablasts upon antigen rechallenge approximately a year

329   after vaccination (27). Further studies will be necessary to understand the implications of CD22

330   upregulation on S-RBD-specific rMBC and intMBC, CXCR5 downregulation on S-RBD-

331   specific atyMBC, and CD38 upregulation on S-RBD-specific actMBC in the mild group but not

332   the severe group, but none of these differences necessarily indicate dysfunction in either group.

333   Overall, despite our lack of longitudinal testing, the phenotypic similarity of S-RBD-specific

334   MBC in this study to typical, germinal center-derived MBC induced by effective vaccination

335   provide strong evidence that these S-RBD-specific MBC are durable and functional.

336   In summary, we have demonstrated that S-RBD-specific class-switched MBC develop in

337   most SARS-CoV-2-infected individuals, including those with mild disease or low levels of

338   plasma anti-S-RBD IgG and neutralizing antibodies. The most abundant subset of S-RBD-

339   specific class-switched MBC in both cohorts were rMBC, and atyMBC were a minor population.

340   FCRL5, a marker of a functional memory response when expressed on antigen-specific rMBC,

341   was dramatically upregulated on S-RBD-specific rMBC, particularly after mild infection. These

342   data indicate that most SARS-CoV-2-infected individuals develop S-RBD-specific, class-

343   switched MBC that phenotypically resemble B cells induced by effective vaccination against

344   other pathogens, providing evidence for durable humoral immunity against SARS-CoV-2 after

345   recovery from either mild or severe COVID-19 disease. These data have implications for risk of

346   reinfection after recovery from COVID-19, and also provide a standard against which B cell

347   responses to novel SARS-CoV-2 vaccines could be compared.

Methods

Study participants

Participants with mild COVID-19 disease who never required hospitalization or supplemental oxygen were identified in a cohort of ambulatory COVID-19 patients. Symptoms in this cohort were tracked using a FLU-PRO score calculated from a participant survey, as previously described (28). Participants with moderate to severe COVID-19 disease were selected from a cohort of hospitalized patients (29), matched with the mild participants based on time since onset of symptoms at the time of blood sampling. PBMC cryopreserved prior to the onset of the COVID-19 pandemic were also obtained from anonymous healthy blood donors. Healthy and COVID-19 participant blood specimens were ficoll gradient separated into plasma and PBMCs. PBMCs were viably cryopreserved in FBS + 10% DMSO for future use.

Expression and purification of soluble Spike protein Receptor Binding Domain (S-RBD)

Plasmid preparation

Recombinant plasmid constructs containing modified S protein Receptor Binding Domain (S-RBD) and a beta-lactamase (amp) gene were obtained (Stadlbauer 2020) and amplified in E.coli after transformation and growth on LB agar plates coated with Ampicillin. The plasmids were extracted using GigaPrep kits (Thermo Fisher Scientific) and eluted in molecular biology grade water.

Recombinant protein expression

HEK293.2sus cells (ATCC) were obtained and adapted to Freestyle™ F-17 medium (Thermo Fisher Scientific) and BalanCD® (Irvine Scientific) using polycarbonate shake flasks

369   (Fisherbrand) with 4mM GlutaMAX supplementation (Thermo Fisher Scientific). The cells were

370   routinely maintained every 4 days at a seeding density of 0.5 million cells/mL. They were

371   cultured at 37°C, 90% humidity with 5% CO2 for cells in BalanCD® while those in F-17 were

372   maintained at 8% CO2. Cells were counted using trypan blue dye (Gibco) exclusion method and

373   a hemocytometer. Cell viability was always maintained above 90%. Twenty-four hours prior to

374   transfection (Day -1), the cells were seeded at a density of 1 million cells/mL, ensuring that the

375   cell viability was above 90%. Polyethylenimine (PEI) stocks, with 25 kDa molecular mass

376   (Polysciences), were prepared in MilliQ water at a concentration of 1 mg/mL. This was filter

377   sterilized through a 0.22 μm syringe filter (Corning), aliquoted and stored at -20°C. On the day

378   of transfection (Day 0), the cells were counted to ensure sufficient growth and viability.

379   OptiPRO™ SFM (Gibco) was used as the medium for transfection mixture. For 100 mL of cell

380   culture, 2 tubes were aliquoted with 6.7 mL each of OptiPRO™, one for PEI and the other for

381   rDNA. DNA:PEI ratio of 1:3.5 was used for transfection. A volume of 350 μL of prepared PEI

382   stock solution was added to tube 1 while 100 μg of rDNA was added to tube 2 and incubated for

383   5 minutes. Post incubation, these were mixed together, incubated for 10 minutes at RT and then

384   added to the culture through gravity addition. The cells were returned back to the 37°C

385   incubator. A day after transfection (Day 1), the cells were spun down at 1,000 rpm for 7 minutes

386   at RT and resuspended in fresh media with GlutaMAX™ supplementation. 3-5 hours after

387   resuspension, 0.22 μm sterile filtered Sodium butyrate (EMD Millipore) was added to the flask at

388   a final concentration of 5 mM (Grünberg et al.). The cells were allowed to grow for a period of

389   4-5 days. Cell counts, viability, glucose and lactate values were measured every day. Cells were

390   harvested when either the viability fell below 60% or when the glucose was depleted, by

391   centrifugation at 5000 rpm for 10 minutes at RT. Cell culture supernatants containing either

392 recombinant S-RBD or S protein were filtered through 0.22 μm PES membrane stericup filters

393 (Millipore Sigma) to remove cell debris and stored at -20°C until purification.

394 Protein purification

395 Protein purification by immobilized metal affinity chromatography (IMAC) and gravity flow

396 was adapted from previous methods (23). After washing with Phosphate-Buffered Saline (PBS;

397 Thermo Fisher Scientific), Nickel-Nitrilotriacetic acid (Ni-NTA) agarose (Qiagen) was added to

398 culture supernatant followed by overnight incubation (12-16 hours) at 4 °C on a rotator. For

399 every 150 mL of culture supernatant, 2.5 mL of Ni-NTA agarose was added. 5mL gravity flow

400 polypropylene columns (Qiagen) were equilibrated with PBS. One polypropylene column was

401 used for every 150 mL of culture supernatant. The supernatant-agarose mixture was then loaded

402 onto the column to retain the agarose beads with recombinant proteins bound to the beads. Each

403 column was then washed, first with 1X culture supernatant volume of PBS and then with 25 mL

404 of 20 mM imidazole (Millipore Sigma) in PBS wash buffer to remove host cell proteins.

405 Recombinant proteins were then eluted from each column in three fractions with 5 mL of 250

406 mM imidazole in PBS elution buffer per fraction giving a total of 15 mL eluate per column. The

407 eluate was subsequently dialyzed several times against PBS using Amicon Ultra Centrifugal

408 Filters (Millipore Sigma) at 7000 rpm for 20 minutes at 10 °C to remove the imidazole and

409 concentrate the eluate. Filters with a 10 kDa molecular weight cut-off were used for S-RBD

410 eluate. The final concentration of the recombinant S-RBD and S proteins was measured by

411 bicinchoninic acid (BCA) assay (Thermo Fisher Scientific), and purity was assessed on 10%

412 SDS-PAGE (Bio-Rad) followed by Coomassie blue staining. After sufficient destaining in water

413 overnight, clear single bands were visible for S-RBD.

414   Viruses and cells.

415   Vero-E6 cells (ATCC CRL-1586) and Vero-E6-TMPRSS2 cells (24) were cultured in

416   Dulbecco's modified Eagle medium (DMEMD) containing 10% fetal bovine serum (Gibco), 1

417   mM glutamine (Invitrogen), 1 mM sodium pyruvate (Invitrogen), 100 U/ml of penicillin

418   (Invitrogen), and 100 μg/ml of streptomycin (Invitrogen) (complete media or CM). Cells were

419   incubated in a 5% CO_2 humidified incubator at 37°C. The SARS-CoV-2/USA-WA1/2020 virus

420   was obtained from BEI Resources. The infectious virus titer was determined on Vero cells using

421   a 50% tissue culture infectious dose (TCID50) assay as previously described for SARS-CoV (25,

422   26). Serial 10-fold dilutions of the virus stock were made in infection media (IM, which is

423   identical to CM except the FBS is reduced to 2.5%), then then 100 μl of each dilution was added

424   to Vero cells in a 96-well plate in sextuplicate. The cells were incubated at 37°C for 4 days,

425   visualized by staining with naphthol blue-black, and scored visually for cytopathic effect. A

426   Reed and Muench calculation was used to determine TCID50 per ml (27).

427   **Measurement of endpoint anti-S-RBD IgG titer.**

428   The protocol was adapted from a published protocol from Dr. Florian Krammer's laboratory

429   (Stadlbauer 2020). Ninety-six well plates (Immulon 4HBX, Thermo Fisher) were coated with S-

430   RBD at a volume of 50 μl of 2 μg/ml of diluted antigen in filtered, sterile 1xPBS (Thermo

431   Fisher) at 4°C overnight. Coating buffer was removed, plates were washed three times with 300

432   μl of PBS-T wash buffer (1xPBS plus 0.1% Tween 20, Fisher Scientific), and blocked with 200

433   μl of PBS-T with 3% non-fat milk (milk powder, American Bio) by volume for one hour at room

434   temperature. All plasma samples were heat inactivated at 56°C on a heating block for one hour

435   prior to use. Negative control samples were prepared at 1:10 dilutions in PBS-T in 1% non-fat

436   milk and plated at a final concentration of 1:100. A monoclonal antibody (mAb) specific for the

437　　SARS-CoV-2 spike protein was used as a positive control (1:5,000, Sino Biological). For serial

438　　dilutions of plasma on S-RBD coated plates, plasma samples were prepared in three-fold serial

439　　dilutions starting at 1:20 in PBST in 1% non-fat-milk. Blocking solution was removed and 10 μl

440　　of diluted plasma was added in duplicates to plates and incubated at room temperature for two

441　　hours. Plates were washed three times with PBS-T wash buffer and 50 μl secondary antibody

442　　was added to plates and incubated at room temperature for one hour. Anti-human secondary

443　　antibodies used included Fc-specific total IgG HRP (1:5,000 dilution, Invitrogen), prepared in

444　　PBS-T plus 1% non-fat milk. Plates were washed and all residual liquid removed before adding

445　　100 μl of SIGMAFAST OPD (o-phenylenediamine dihydrochloride) solution (Sigma Aldrich) to

446　　each well, followed by incubation in darkness at room temperature for ten minutes. To stop the

447　　reaction, 50 μl of 3M hydrochloric acid (HCl, Fisher Scientific) was added to each well. The OD

448　　of each plate was read at 490nm (OD490) on a SpectraMax i3 ELISA plate reader (BioTek). The

449　　positive cutoff value for each plate was calculated by summing the average of the negative

450　　values and three times the standard deviation of the negatives. All values at or above the cutoff

451　　value were considered positive. Values were graphed on a dose response curve, a best fit line

452　　drawn by nonlinear regression, and area under the curve (AUC) calculated.

453　　**Measurement of endpoint neutralization titer.**

454　　Plasma neutralization titers were determined as described for SARS-CoV (Schaecher 2008).

455　　Two-fold dilutions of plasma (starting at a 1:20 dilution) were made in IM. Infectious virus was

456　　added to the plasma dilutions at a final concentration of 1x104 TCID50/ml (100 TCID50 per

457　　100ul). The samples were incubated for one hour at room temperature, then 100 uL of each

458　　dilution was added to one well of a 96 well plate of VeroE6-TMPRSS2 cells in sextuplet for 6

459　　hours at 37°C. The inoculums were removed, fresh IM was added, and the plates were incubated

460   at 37°C for 2 days. The cells were fixed by the addition of 150 uL of 4% formaldehyde per well,

461   incubated for at least 4 hours at room temperature, then stained with Napthol blue black. The

462   nAb titer was calculated as the highest serum dilution that eliminated cytopathic effect (CPE) in

463   50% of the wells. Values were graphed on a dose response curve, a best fit line drawn by

464   nonlinear regression, and area under the curve (AUC) calculated.

465   **Cell staining and flow cytometry**

466   PBMCs were isolated from blood using ficoll separation gradient and viably frozen. Cells were

467   thawed before use, and 5e6-10e6 PBMCs were stained from each participant. Fc blocker (BD

468   Cat #564220) diluted in FACS Buffer (1x PBS with 1% BSA) was added to the cells and

469   incubated for 30minutes on ice or 4c. The cells were then washed twice with FACS buffer.

470   Soluble 6X-His tagged S-RBD protein was then added to the cells and incubated at room

471   temperature for 30 min. This was followed by wash steps with FACS buffer. Conjugated

472   antibodies (Suppl. Table 1 for list of antibodies and their conjugate fluorophores) and live dead

473   stain was then added to the cells and incubated for an additional 30min. The cells were washed

474   two or three more times before running the cells on BD Biosciences LSR II instrument. 1e6-6e6

475   total events were collected for each participant, resulting in medians of 69.5 absolute RBD+ and

476   13,971 RBD- class switched MBC for each participant (range=1-454 RBD+, 152-84,645 RBD-

477   MBC). For UMAP analysis, all RBD+ class switched MBC were included, and RBD- class

478   switched MBC were downsampled to 3000 cells per subject. The subject with only 1 RBD+ cell

479   was excluded from RBD+ MBC subset analyses. Positive gates for each fluorophore were set

480   after compensation and using fluorescence minus one (FMO) staining and isotype control

481   antibodies.

482   **Statistical analysis**

483   FlowJo software was used to analyze all the flow results from the LSRII. Statistical analyses

484   were performed in Prism (Graphpad software). Two group comparisons were performed with t

485   tests if data were normally distributed based on Shapiro Wilk normality test or Mann Whitney

486   rank test if data were not normally distributed. Multi-group comparisons were performed using

487   one-way ANOVA, with p values adjusted for multiple comparisons using the Benjamini, Krieger

488   and Yekutieli method.

489   **Study approval.**

490   This research was approved by the Johns Hopkins University School of Medicine's Institutional

491   Review Board (IRB). Prior to blood collection, all participants provided informed written

492   consent.

493

494

495

Author Contributions. COO conceived the project, performed experiments, interpreted data, and wrote the initial manuscript draft; NES conceived the project, performed experiments, and interpreted data; PWB interpreted data; HSP, KL, and AG performed experiments and interpreted data; AA interpreted data; SCR interpreted data; PL and MJB provided reagents. AP performed experiments and interpreted data; SLK performed experiments and interpreted data; YCM conceived the project and provided participant samples; ALC conceived the project, provided participant samples, and interpreted data; JRB conceived the project, interpreted data, and wrote the initial manuscript draft. All authors reviewed and edited the manuscript.

515   References

516   1.   Guan WJ, and Zhong NS. Clinical Characteristics of Covid-19 in China. Reply. *N Engl J*
517   *Med.* 2020;382(19):1861-2.
518   2.   Wang Z, Yang B, Li Q, Wen L, and Zhang R. Clinical Features of 69 Cases With
519   Coronavirus Disease 2019 in Wuhan, China. *Clin Infect Dis.* 2020;71(15):769-77.
520   3.   Long QX, Liu BZ, Deng HJ, Wu GC, Deng K, Chen YK, Liao P, Qiu JF, Lin Y, Cai XF,
521   et al. Antibody responses to SARS-CoV-2 in patients with COVID-19. *Nat Med.* 2020.
522   4.   Seow J, Graham C, Merrick B, Acors S, Steel KJA, Hemmings O, O'Bryne A, Kouphou
523   N, Pickering S, Galao R, et al. Longitudinal evaluation and decline of antibody responses
524   in SARS-CoV-2 infection. *medRxiv.* 2020:2020.07.09.20148429.
525   5.   Ibarrondo FJ, Fulcher JA, Goodman-Meza D, Elliott J, Hofmann C, Hausner MA, Ferbas
526   KG, Tobin NH, Aldrovandi GM, and Yang OO. Rapid Decay of Anti-SARS-CoV-2
527   Antibodies in Persons with Mild Covid-19. *N Engl J Med.* 2020;383(11):1085-7.
528   6.   Patel MM, Thornburg NJ, Stubblefield WB, Talbot HK, Coughlin MM, Feldstein LR,
529   and Self WH. Change in Antibodies to SARS-CoV-2 Over 60 Days Among Health Care
530   Personnel in Nashville, Tennessee. *JAMA.* 2020.
531   7.   Wajnberg A, Amanat F, Firpo A, Altman D, Bailey M, Mansour M, McMahon M, Meade
532   P, Mendu DR, Muellers K, et al. SARS-CoV-2 infection induces robust, neutralizing
533   antibody responses that are stable for at least three months. *medRxiv.*
534   2020:2020.07.14.20151126.
535   8.   Isho B, Abe KT, Zuo M, Jamal AJ, Rathod B, Wang JH, Li Z, Chao G, Rojas OL, Bang
536   YM, et al. Persistence of serum and saliva antibody responses to SARS-CoV-2 spike
537   antigens in COVID-19 patients. *Sci Immunol.* 2020;5(52).
538   9.   Iyer AS, Jones FK, Nodoushani A, Kelly M, Becker M, Slater D, Mills R, Teng E,
539   Kamruzzaman M, Garcia-Beltran WF, et al. Persistence and decay of human antibody
540   responses to the receptor binding domain of SARS-CoV-2 spike protein in COVID-19
541   patients. *Sci Immunol.* 2020;5(52).
542   10.   Klein SL, Pekosz A, Park HS, Ursin RL, Shapiro JR, Benner SE, Littlefield K, Kumar S,
543   Naik HM, Betenbaugh MJ, et al. Sex, age, and hospitalization drive antibody responses in
544   a COVID-19 convalescent plasma donor population. *J Clin Invest.* 2020.
545   11.   Salimzadeh L, Le Bert N, Dutertre CA, Gill US, Newell EW, Frey C, Hung M, Novikov
546   N, Fletcher S, Kennedy PT, et al. PD-1 blockade partially recovers dysfunctional virus-
547   specific B cells in chronic hepatitis B infection. *J Clin Invest.* 2018;128(10):4573-87.
548   12.   Middleman AB, Baker CJ, Kozinetz CA, Kamili S, Nguyen C, Hu DJ, and Spradling PR.
549   Duration of protection after infant hepatitis B vaccination series. *Pediatrics.*
550   2014;133(6):e1500-7.
551   13.   Kaneko N, Kuo HH, Boucau J, Farmer JR, Allard-Chamard H, Mahajan VS, Piechocka-
552   Trocha A, Lefteri K, Osborn M, Bals J, et al. Loss of Bcl-6-Expressing T Follicular
553   Helper Cells and Germinal Centers in COVID-19. *Cell.* 2020;183(1):143-57 e13.
554   14.   Robbiani DF, Gaebler C, Muecksch F, Lorenzi JCC, Wang Z, Cho A, Agudelo M,
555   Barnes CO, Gazumyan A, Finkin S, et al. Convergent antibody responses to SARS-CoV-
556   2 in convalescent individuals. *Nature.* 2020;584(7821):437-42.
557   15.   Zost SJ, Gilchuk P, Case JB, Binshtein E, Chen RE, Nkolola JP, Schafer A, Reidy JX,
558   Trivette A, Nargi RS, et al. Potently neutralizing and protective human antibodies against
559   SARS-CoV-2. *Nature.* 2020;584(7821):443-9.

16. Noy-Porat T, Makdasi E, Alcalay R, Mechaly A, Levy Y, Bercovich-Kinori A, Zauberman A, Tamir H, Yahalom-Ronen Y, Israeli M, et al. A panel of human neutralizing mAbs targeting SARS-CoV-2 spike at multiple epitopes. *Nat Commun.* 2020;11(1):4303.

17. Rogers TF, Zhao F, Huang D, Beutler N, Burns A, He WT, Limbo O, Smith C, Song G, Woehl J, et al. Isolation of potent SARS-CoV-2 neutralizing antibodies and protection from disease in a small animal model. *Science.* 2020;369(6506):956-63.

18. Brouwer PJM, Caniels TG, van der Straten K, Snitselaar JL, Aldon Y, Bangaru S, Torres JL, Okba NMA, Claireaux M, Kerster G, et al. Potent neutralizing antibodies from COVID-19 patients define multiple targets of vulnerability. *Science.* 2020;369(6504):643-50.

19. Buchholz UJ, Bukreyev A, Yang L, Lamirande EW, Murphy BR, Subbarao K, and Collins PL. Contributions of the structural proteins of severe acute respiratory syndrome coronavirus to protective immunity. *Proc Natl Acad Sci U S A.* 2004;101(26):9804-9.

20. Du L, He Y, Zhou Y, Liu S, Zheng BJ, and Jiang S. The spike protein of SARS-CoV--a target for vaccine and therapeutic development. *Nat Rev Microbiol.* 2009;7(3):226-36.

21. Li T, Xie J, He Y, Fan H, Baril L, Qiu Z, Han Y, Xu W, Zhang W, You H, et al. Long-term persistence of robust antibody and cytotoxic T cell responses in recovered patients infected with SARS coronavirus. *PLoS One.* 2006;1(e24.

22. Huang AT, Garcia-Carreras B, Hitchings MDT, Yang B, Katzelnick L, Rattigan SM, Borgert B, Moreno C, Solomon BD, Rodriguez-Barraquer I, et al. A systematic review of antibody mediated immunity to coronaviruses: antibody kinetics, correlates of protection, and association of antibody responses with severity of disease. *medRxiv.* 2020:2020.04.14.20065771.

23. Deng W, Bao L, Liu J, Xiao C, Liu J, Xue J, Lv Q, Qi F, Gao H, Yu P, et al. Primary exposure to SARS-CoV-2 protects against reinfection in rhesus macaques. *Science.* 2020;369(6505):818-23.

24. Chandrashekar A, Liu J, Martinot AJ, McMahan K, Mercado NB, Peter L, Tostanoski LH, Yu J, Maliga Z, Nekorchuk M, et al. SARS-CoV-2 infection protects against rechallenge in rhesus macaques. *Science.* 2020;369(6505):812-7.

25. Moir S, Ho J, Malaspina A, Wang W, DiPoto AC, O'Shea MA, Roby G, Kottilil S, Arthos J, Proschan MA, et al. Evidence for HIV-associated B cell exhaustion in a dysfunctional memory B cell compartment in HIV-infected viremic individuals. *J Exp Med.* 2008;205(8):1797-805.

26. Kim CC, Baccarella AM, Bayat A, Pepper M, and Fontana MF. FCRL5(+) Memory B Cells Exhibit Robust Recall Responses. *Cell Rep.* 2019;27(5):1446-60 e4.

27. Nellore A, Scharer CD, King RG, Tipton CM, Zumaquero E, Fucile C, Mousseau B, Bradley JE, Macon K, Mi T, et al. Fcrl5 and T-bet define influenza-specific memory B cells that predict long-lived antibody responses. *bioRxiv.* 2019:643973.

28. Blair PW, Brown DM, Jang M, Antar AA, Keruly JC, Bachu V, Townsend JL, Tornheim JA, Keller SC, Sauer L, et al. The clinical course of COVID-19 in the outpatient setting: a prospective cohort study. *medRxiv.* 2020:2020.09.01.20184937.

29. Thompson EA, Cascino K, Ordonez AA, Zhou W, Vaghasia A, Hamacher-Brady A, Brady NR, Sun I-H, Wang R, Rosenberg AZ, et al. Metabolic programs define dysfunctional immune responses in severe COVID-19 patients. *medRxiv.* 2020:2020.09.10.20186064.

606   30.   Crocker PR, Paulson JC, and Varki A. Siglecs and their roles in the immune system.
607   *Nature Reviews Immunology.* 2007;7(4):255-66.
608   31.   Macauley MS, Crocker PR, and Paulson JC. Siglec-mediated regulation of immune cell
609   function in disease. *Nature Reviews Immunology.* 2014;14(10):653-66.
610   32.   Tateno H, Li H, Schur MJ, Bovin N, Crocker PR, Wakarchuk WW, and Paulson JC.
611   Distinct endocytic mechanisms of CD22 (Siglec-2) and Siglec-F reflect roles in cell
612   signaling and innate immunity. *Mol Cell Biol.* 2007;27(16):5699-710.
613   33.   Watanabe N, Gavrieli M, Sedy JR, Yang J, Fallarino F, Loftin SK, Hurchla MA,
614   Zimmerman N, Sim J, Zang X, et al. BTLA is a lymphocyte inhibitory receptor with
615   similarities to CTLA-4 and PD-1. *NatImmunol.* 2003;4(670-9.
616   34.   Davis RS. FCRL regulation in innate-like B cells. *Ann N Y Acad Sci.* 2015;1362(1):110-
617   6.
618   35.   Liao HX, Lynch R, Zhou T, Gao F, Alam SM, Boyd SD, Fire AZ, Roskin KM, Schramm
619   CA, Zhang Z, et al. Co-evolution of a broadly neutralizing HIV-1 antibody and founder
620   virus. *Nature.* 2013;496(7446):469-76.
621   36.   Hardtke S, Ohl L, and Förster R. Balanced expression of CXCR5 and CCR7 on follicular
622   T helper cells determines their transient positioning to lymph node follicles and is
623   essential for efficient B-cell help. *Blood.* 2005;106(6):1924-31.
624   37.   Junt T, Fink K, Förster R, Senn B, Lipp M, Muramatsu M, Zinkernagel RM, Ludewig B,
625   and Hengartner H. CXCR5-Dependent Seeding of Follicular Niches by B and Th Cells
626   Augments Antiviral B Cell Responses. *The Journal of Immunology.* 2005;175(11):7109-
627   16.
628   38.   Sanz I, Wei C, Lee FE, and Anolik J. Phenotypic and functional heterogeneity of human
629   memory B cells. *Semin Immunol.* 2008;20(1):67-82.
630   39.   Lau D, Lan LY, Andrews SF, Henry C, Rojas KT, Neu KE, Huang M, Huang Y,
631   DeKosky B, Palm AE, et al. Low CD21 expression defines a population of recent
632   germinal center graduates primed for plasma cell differentiation. *Sci Immunol.* 2017;2(7).
633   40.   Joosten SA, van Meijgaarden KE, Del Nonno F, Baiocchini A, Petrone L, Vanini V,
634   Smits HH, Palmieri F, Goletti D, and Ottenhoff TH. Patients with Tuberculosis Have a
635   Dysfunctional Circulating B-Cell Compartment, Which Normalizes following Successful
636   Treatment. *PLoS Pathog.* 2016;12(6):e1005687.
637   41.   Portugal S, Tipton CM, Sohn H, Kone Y, Wang J, Li S, Skinner J, Virtaneva K,
638   Sturdevant DE, Porcella SF, et al. Malaria-associated atypical memory B cells exhibit
639   markedly reduced B cell receptor signaling and effector function. *Elife.* 2015;4(
640   42.   Oliviero B, Varchetta S, Mele D, Mantovani S, Cerino A, Perotti CG, Ludovisi S, and
641   Mondelli MU. Expansion of atypical memory B cells is a prominent feature of COVID-
642   19. *Cell Mol Immunol.* 2020;17(10):1101-3.
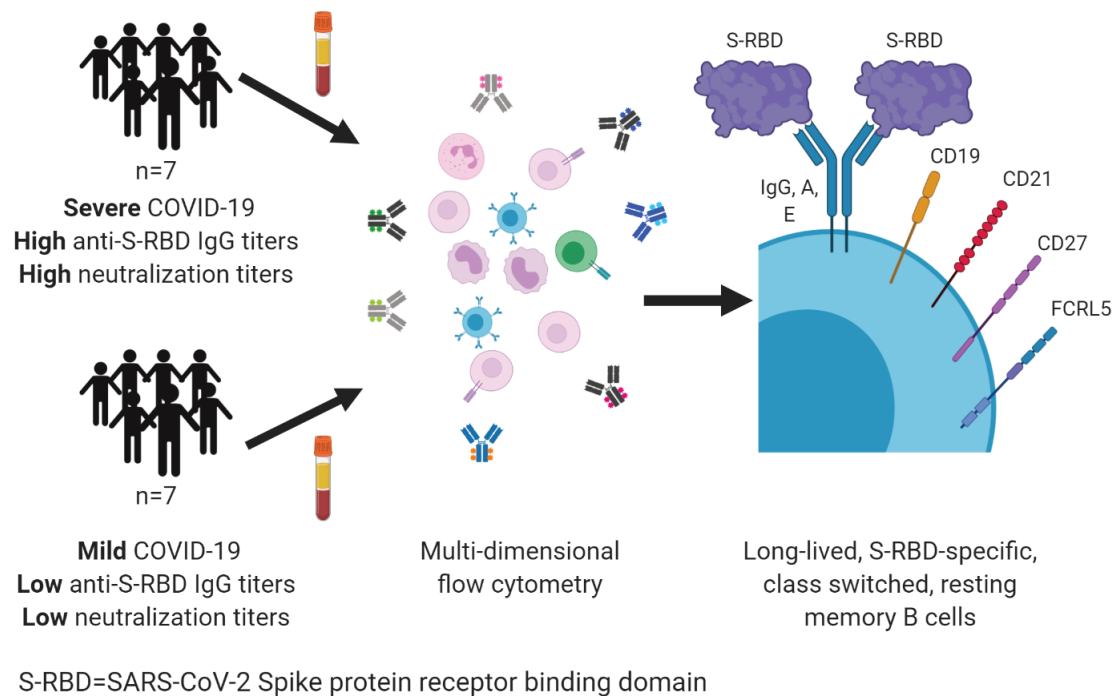
643

Graphical Abstract

S-RBD=SARS-CoV-2 Spike protein receptor binding domain

Table 1. Participant characteristics

Participant ID	Age[1]	Sex	Race	Ethnicity	Days from symptom onset	FLU-PRO[2]	Supp. O$_2$[3]
Mild-ambulatory							
M1	60	F	White	Non-Hispanic	63	0.38	none
M2	50	F	Hawaiian/Pacific Islander	Non-Hispanic	68	0.28	none
M3	60	F	White	Hispanic	59	0.19	none
M4	70	F	White	Non-Hispanic	64	0.06	none
M5	60	M	White	Non-Hispanic	46	0	none
M6	40	M	Black	Non-Hispanic	61	0.03	none
M7	30	M	American Indian/Alaska Native	Non-Hispanic	45	0.09	none
median	*60*				*61*	*0.09*	
Severe-hospitalized							
S1	70	F	Black	Non-Hispanic	90	n/a	4LNC
S2	50	M	Black	Non-Hispanic	104	n/a	HFNC
S3	60	M	White	Non-Hispanic	48	n/a	Intubated
S4	50	M	Other	Non-Hispanic	46	n/a	2LNC
S5	80	F	Black	Non-Hispanic	39	n/a	Intubated
S6	50	M	Black	Non-Hispanic	42	n/a	HFNC
S7	70	M	Other	Non-Hispanic	41	n/a	Intubated
median	*60*				*46*		

[1]Age rounded to nearest 10 to avoid identifying participants. [2]Peak FLU-PRO score. [3]Maximum oxygen support required. 4LNC, 4 liters via nasal cannula; HFNC, high flow oxygen via nasal cannula; intubated, requiring mechanical ventilation; 2LNC, 2 liters via nasal cannula.
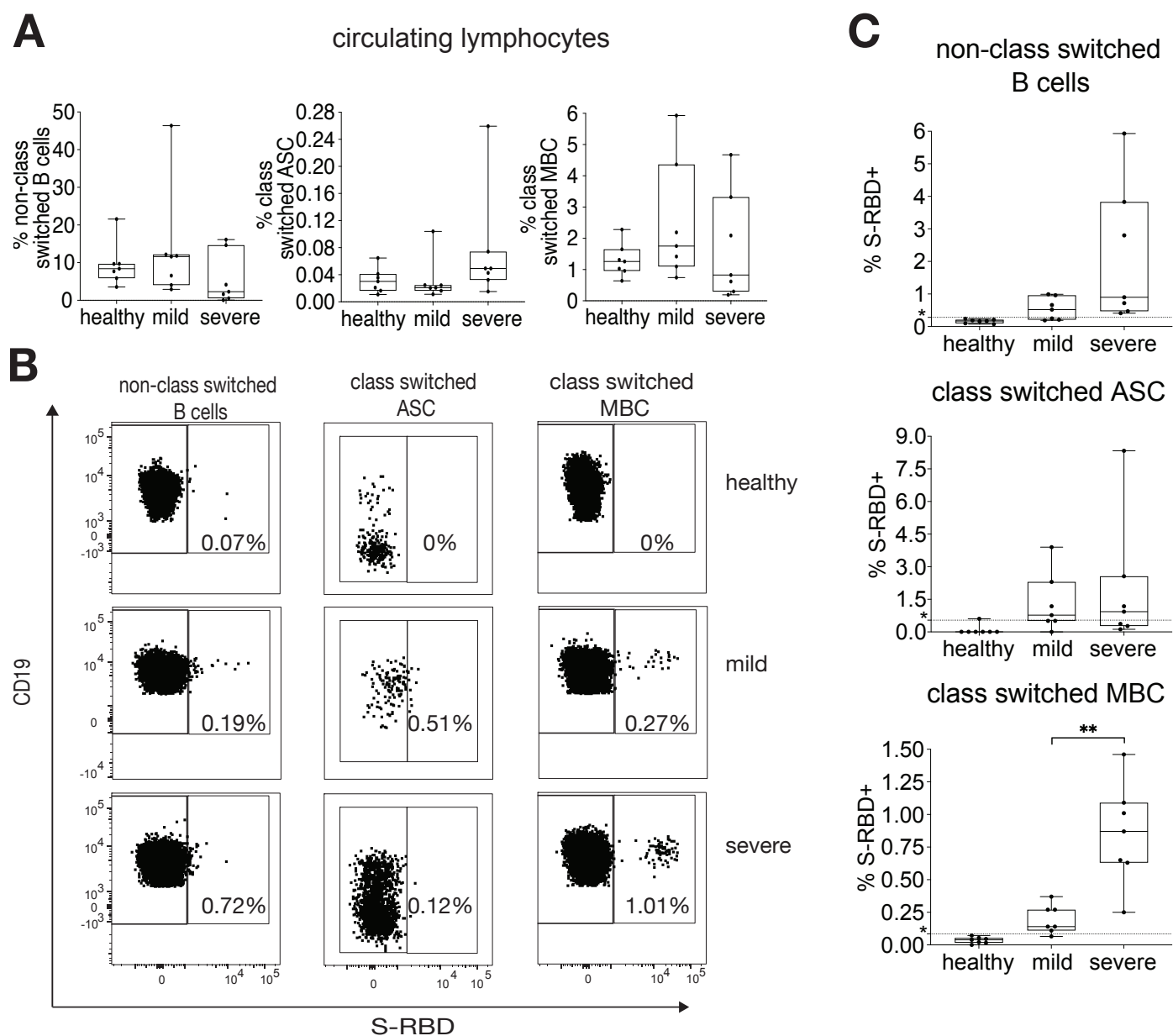
Figure 1. Quantifying S-RBD specific B cells. (A) % of lymphocytes that are class switched MBC, class switched ASC, or non-class switched B cells in healthy, mild, and severe participants (N=7 for each group). **(B)** Gating strategy for S-RBD specific non-class switched B cells (CD3-, CD19+, IgD/IgM+, S-RBD+), S-RBD specific class switched MBC (CD3-, CD19+, IgM-, IgD-, CD38+/- (excluding ++), CD138-, S-RBD+), and S-RBD specific class switched ASC (CD3-, CD19+/-, IgM-, IgD-, CD38++, CD27+, S-RBD+) in "healthy" (COVID-19 negative), "mild" (COVID-19+, ambulatory), and "severe" (COVID-19+, hospitalized) participants. **(C)** % of class switched MBC, class switched ASC, and non-class switched B cells that are S-RBD specific in healthy, mild, and severe participants (N=7 for each group). Dotted line represents the true positive threshold, defined as the mean plus two standard deviations of the healthy group. For **A and C** box plots, horizontal lines indicate means, boxes are inter-quartile range, and whiskers are minimum to maximum. Three group comparisons in **A** were performed using one-way ANOVA, with p values adjusted for multiple comparisons using the Benjamini, Krieger and Yekutieli method. Two group comparisons in **C** were performed with t tests if data were normally distributed based on Shapiro Wilk normality test or Mann Whitney test if data were not normally distributed. Statistically significant comparisons are indicated (** $P \leq 0.01$)
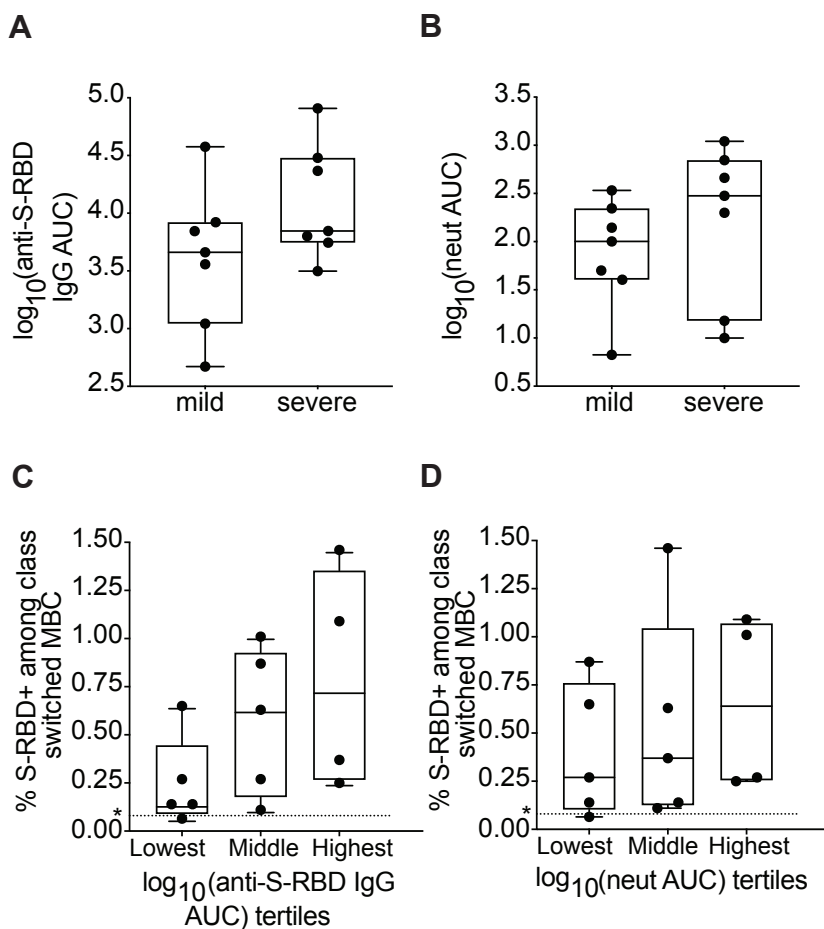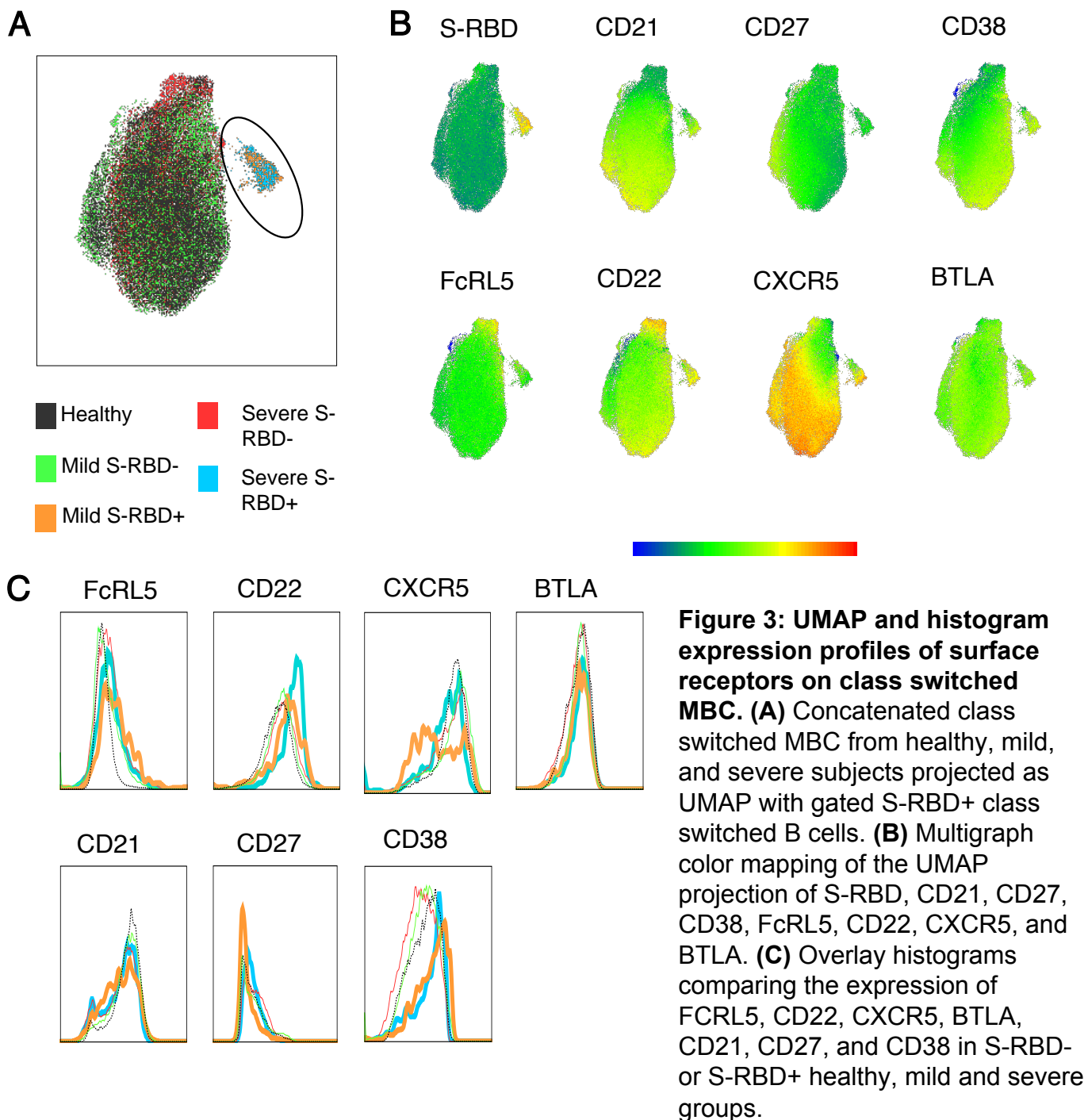
Figure 2. Comparisons of serum anti S-RBD IgG and neutralizing antibody titers in mild and severe participants. (A) Anti S-RBD IgG area under the curve (AUC) in mild and severe participants. **(B)** Neutralizing antibody AUC in mild and severe participants. **(C)** % of class switched MBC that are RBD specific, from participants with plasma anti-S-RBD AUC values in the lowest, middle, and highest tertiles. **(D)** % of class switched MBC that are RBD specific, from participants with plasma neutralizing antibody AUC values in the lowest, middle, and highest tertiles. Dotted line represents the true positive threshold, defined as the mean plus two standard deviations of the healthy group. For box plots, horizontal lines indicate means, boxes are inter-quartile range, and whiskers are minimum to maximum. P values for **A-B** were calculated using t tests and P values for **C-D** were calculated using one-way ANOVA test for linear trend. No statistically significant comparison was found.
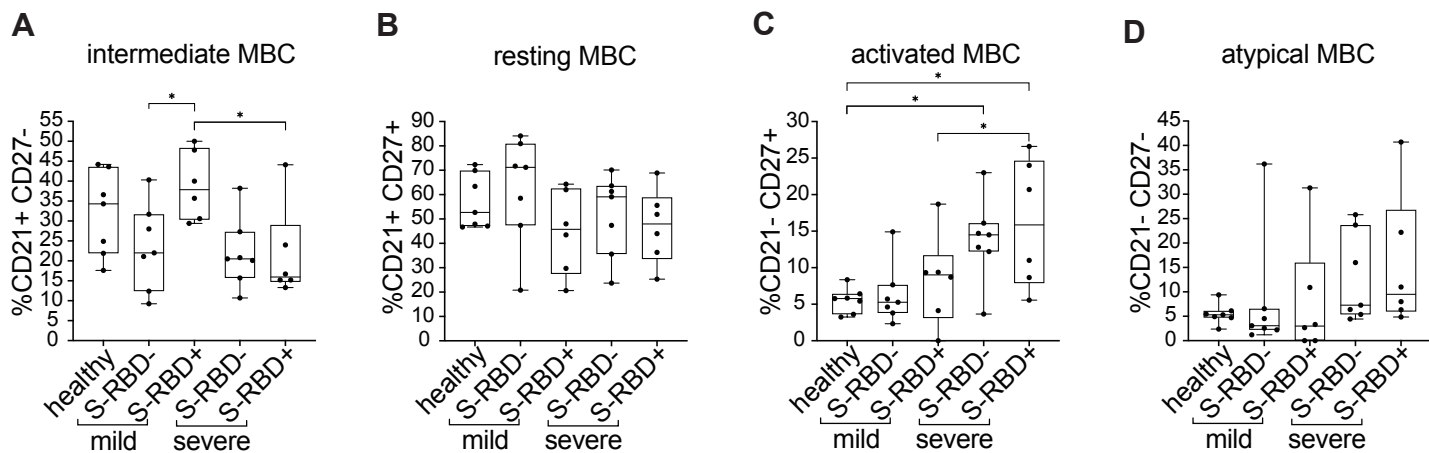
Figure 3: UMAP and histogram expression profiles of surface receptors on class switched MBC. (A) Concatenated class switched MBC from healthy, mild, and severe subjects projected as UMAP with gated S-RBD+ class switched B cells. **(B)** Multigraph color mapping of the UMAP projection of S-RBD, CD21, CD27, CD38, FcRL5, CD22, CXCR5, and BTLA. **(C)** Overlay histograms comparing the expression of FCRL5, CD22, CXCR5, BTLA, CD21, CD27, and CD38 in S-RBD- or S-RBD+ healthy, mild and severe groups.

Figure 4: Frequency of MBC subsets in S-RBD nonspecific (S-RBD-) or S-RBD specific (S-RB-D+) class switched MBC from healthy, mild, or severe participants. (A) intMBC (CD21+, CD27-). **(B)** rMBC (CD21+, CD27+). **(C)** actMBC (CD21-, CD27+). **(D)** atyMBC (CD21-, CD27-). For box plots, horizontal lines indicate means, boxes are inter-quartile range, and whiskers are minimum to maximum. Groups were compared by one-way ANOVA with p values adjusted for multiple comparisons using the Benjamini, Krieger and Yekutieli method. Statistically significant comparisons are indicated (* P ≤ 0.05).
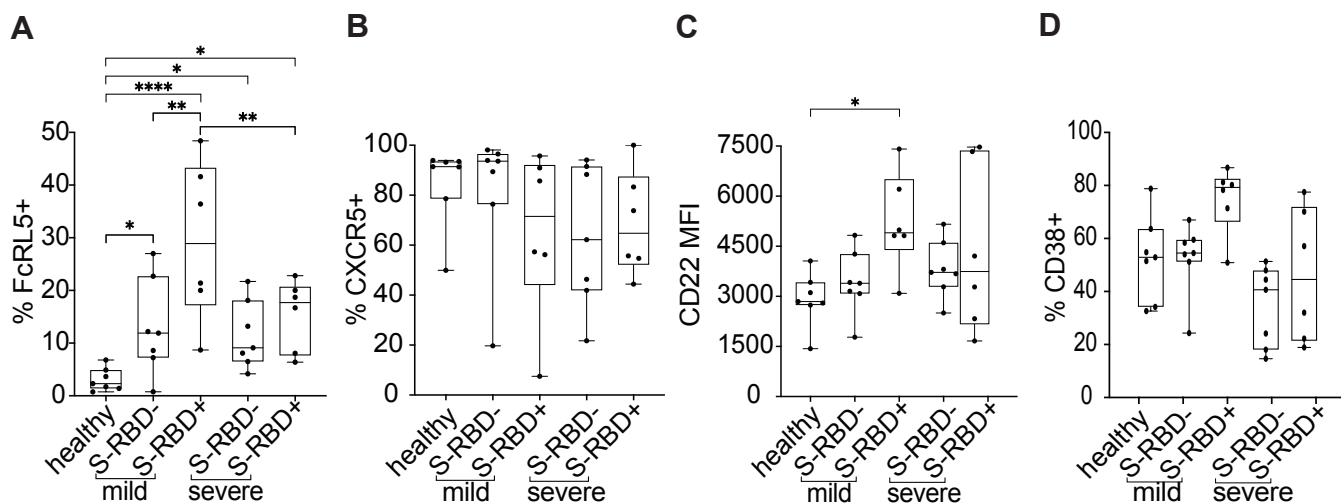
Figure 5: Surface expression of FcRL5, CXCR5, CD22, and CD38 on S-RBD nonspecific (S-RBD-) or S-RBD specific (S-RBD+) class switched MBC from healthy, mild, or severe participants. Expression is shown as either percent of cells positive or the mean fluorescent intensity (MFI). (A) FcRL5 **(B)** CXCR5 **(C)** CD22 **(D)** CD38. For box plots, horizontal lines indicate means, boxes are inter-quartile range, and whiskers are minimum to maximum. Groups were compared by one-way ANOVA with p values adjusted for multiple comparisons using the Benjamini, Krieger and Yekutieli method. Statistically significant comparisons are indicated (* P ≤ 0.05, ** P ≤ 0.01, *** P ≤ 0.001, **** P ≤ 0.0001).
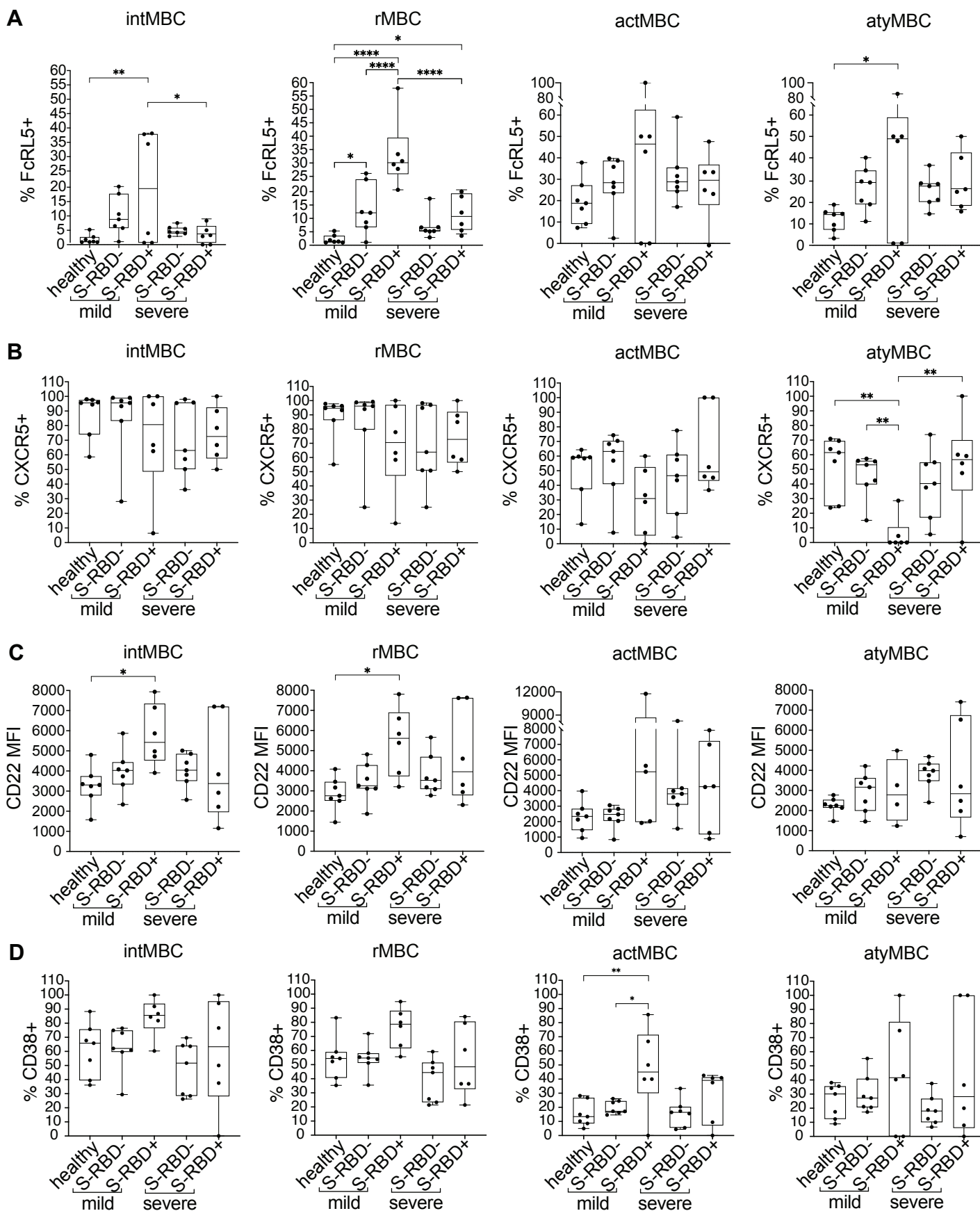
Figure 6: Surface expression of FcRL5, CXCR5, CD22, and CD38 on S-RBD nonspecific (S-RBD-) or S-RBD specific (S-RBD+) class switched intMBC, rMBC, actMBC, or atyMBC from healthy, mild, or severe participants. Expression is shown as either percent of cells positive or the mean fluorescent intensity (MFI). (A) FcRL5 **(B)** CXCR5 **(C)** CD22 **(D)** CD38. For box plots, horizontal lines indicate means, boxes are inter-quartile range, and whiskers are minimum to maximum. Groups were compared by one-way ANOVA with p values adjusted for multiple comparisons using the Benjamini, Krieger and Yekutieli method. Statistically significant comparisons are indicated (* P ≤ 0.05, ** P ≤ 0.01, *** P ≤ 0.001, **** P ≤ 0.0001).